Exp.-Nr. **A2-02/09**
Eingang: 15.05.2009
an PAC: 18.05.2009

Mainz Microtron MAMI

Collaboration A2: "Tagged Photons"
Spokesperson: A. Thomas

Proposal for an Experiment

"Decays of the η' Meson"

Spokespersons for the Experiment :
M. Unverzagt (Institut für Kernphysik, University of Mainz, Germany),
A. Denig (Institut für Kernphysik, University of Mainz, Germany),
B.M.K. Nefkens (University of California, Los Angeles, USA),
A. Starostin (University of California, Los Angeles, USA)

Abstract of Physics :

We propose to perform high–statistics measurements of η' decays, with the emphasis on completely neutral final states. The main focus will be the study of the $\eta' \to \eta\pi^0\pi^0$, $\eta' \to 3\pi^0$ and $\eta' \to \gamma\gamma$ decays. For the decays into three pseudoscalar mesons the shape of the Dalitz plots will be investigated, which provide information about the the $\pi\pi$ and, eventually, the $\pi\eta$ scattering lengths. The shape of the $\eta' \to \eta\pi^0\pi^0$ decay should exhibit a clear cusp effect due to $\pi\pi$ rescattering. The expected statistics of about $4 \cdot 10^5$ $\eta' \to \eta\pi^0\pi^0$ events in 600 hours of data taking exceeds the existing world data sample by more than a factor of 25. Furthermore, we will test C–invariance improving the upper limits of the $\eta' \to \pi^0 e^+e^-$, $\eta' \to \eta e^+e^-$ and $\eta' \to 3\gamma$ C–forbidden decays by more than one order of magnitude. We will also test CP–invariance searching for the $\eta' \to 4\pi^0$ decay, lepton–family violation in the $\eta' \to e\mu$ decay and second class weak interactions in $\eta' \nrightarrow \pi^0 l\nu$ as well as $\eta' \nrightarrow \pi^0 \mu e$.

Abstract of Equipment :

We will use the high–intensity Bremsstrahlung photon beam in the A2 hall with the maximum energy of $E_\gamma^{max} = 1.558\,\mathrm{MeV}$ incident on a 10 cm liquid hydrogen target. For energy tagging of the photons we will use a newly developed end–point tagging device. The almost hermetic detector setup consists of the self–triggering multiphoton spectrometer Crystal Ball and the TAPS wall consisting of BaF_2 and $PbWO_4$ crystals, covering the forward direction. The Crystal Ball will be equipped with the scintillator barrel PID 2 around the lH_2 target.

MAMI Specifications :

beam energy	1558 MeV
beam current	< 40 nA
beam polarisation	unpolarised

Photon Beam Specifications :

tagged energy range	1400 - 1550 MeV (end–point tagger)
photon beam polarisation	unpolarised

Equipment Specifications :

detectors	Crystal Ball, TAPS, PID 2
target	10 cm lH_2

Beam Time Request :

set–up/tests with beam	50 hours
data taking	600 hours
empty target, background	200 hours

List of participating authors:

- **Institut für Physik, University of Basel, Switzerland**
  I. Jaegle, I. Keshelashvili, B. Krusche, Y. Maghrbi, F. Pheron, T. Rostomyan, D. Werthmüller
- **Institut für Experimentalphysik, University of Bochum, Germany**
  W. Meyer, G. Reicherz
- **Helmholtz–Institut für Strahlen- und Kernphysik, University of Bonn, Germany**
  R. Beck, A. Nikolaev
- **Massachusetts Institute of Technology, Cambridge, USA**
  A. Bernstein, W. Deconinck
- **JINR, Dubna, Russia**
  N. Borisov, A. Lazarev, A. Neganov, Yu.A. Usov
- **School of Physics, University of Edinburgh, UK**
  D. Branford, D.I. Glazier, T. Jude, M. Sikora, D.P. Watts
- **Petersburg Nuclear Physics Institute, Gatchina, Russia**
  V. Bekrenev, S. Kruglov, A. Koulbardis
- **Department of Physics and Astronomy, University of Glasgow, UK**
  J.R.M. Annand, D. Hamilton, D. Howdle, K. Livingston, J. Mancell, J.C. McGeorge, I.J.D. MacGregor, E.F. McNicoll, R.O. Owens, J. Robinson, G. Rosner
- **Department of Astronomy and Physics, Saint Mary's University Halifax, Canada**
  A.J. Sarty
- **Kent State University, Kent, USA**
  D.M. Manley
- **University of California, Los Angeles, USA**
  B.M.K. Nefkens, S. Prakhov, A. Starostin, I.M. Suarez
- **MAX-lab, University of Lund, Sweden**
  L. Isaksson
- **Institut für Kernphysik, University of Mainz, Germany**
  P. Aguar-Bartolome, H.J. Arends, S. Bender, A. Denig, E.J. Downie, N. Frömmgen, E. Heid, O. Jahn, H. Ortega, M. Ostrick, B. Oussena, P.B. Otte, S. Schumann, A. Thomas, M. Unverzagt
- **Institut für Physik, University of Mainz, D**
  J. Krimmer, W. Heil
- **University of Massachusetts, Amherst, USA**
  P. Martel, R. Miskimen
- **Institute for Nuclear Research, Moscow, Russia**
  G. Gurevic, R. Kondratiev, V. Lisin, A. Polonski
- **Lebedev Physical Institute, Moscow, Russia**
  S.N. Cherepnya, L.V. Fil kov, V.L. Kashevarov
- **INFN Sezione di Pavia, Pavia, Italy**
  A. Braghieri, A. Mushkarenkov, P. Pedroni
- **Department of Physics, University of Regina, Canada**
  G.M. Huber
- **Mount Allison University, Sackville, Canada**
  D. Hornidge
- **Tomsk Polytechnic University, Tomsk, Russia**
  A. Fix

- **Physikalisches Institut, University of Tübingen, Germany**
  P. Grabmayr, T. Hehl, D.G. Middleton
- **George Washington University, Washington, USA**
  W. Briscoe, T. Morrison, B. Oussena, B. Taddesse, M. Taragin
- **Catholic University, Washington, USA**
  D. Sober
- **Rudjer Boskovic Institute, Zagreb, Croatia**
  M. Korolija, D. Mekterovic, S. Micanovic, I. Supek

1 Introduction

The decays of the η and η' mesons provide unique information on the understanding of low-energy Quantum Chromo Dynamics (QCD), the field theory of strong interaction. Since perturbative QCD cannot be applied in the low-energy region, because the strong coupling constant α_s is large, other methods like lattice QCD, chiral perturbation theory (χPT) or model-depending approaches are used. Decays of the η' can be used to test the applicability of χPT (the η' mass is of the order of the chiral symmetry breaking scale of $4\pi f_\pi \simeq 1.2\,\mathrm{GeV}$). Moreover, many models and theories of hadron interaction can be tested. One can also search for the violation of lepton–family number and place limits on the masses and couplings of many proposed lepto–quark families, see refs [1, 2, 3, 4, 5]. Decays of the η' are also suitable to search for violations of C, CP, and CPT invariance [6].
The decays of the η' meson have been explored only with very limited statistics so far. For the most prominent neutral decay $\eta' \to \eta\pi^0\pi^0$, with a branching ratio of (20.7 ± 1.2) %, the GAMS collaboration very recently published a result based on $15 \cdot 10^3$ events [7]. This represents currently the highest available statistics for this decay. For the $\eta' \to 3\pi^0$ decay with a branching ratio of $(1.54 \pm 0.26) \cdot 10^{-3}$ the GAMS collaboration presented the worlds highest statistics with 235 ± 45 events [8]. It is very crucial to further investigate the η' decays with high statistics. Especially, existing experimental data on η' photoproduction are rather scarce, as can be seen in fig. 1.
We propose to perform measurements of η' decays with the Crystal Ball detector at the Bremsstrahlung facility of the electron accelerator MAMI. Our emphasis will be on the investigation of the main neutral decay channels of the η' meson. Among these is the decay

$$\eta' \to \eta\pi^0\pi^0. \tag{1}$$

It offers the possibility to study the $\pi\pi$ and, hopefully, the $\pi\eta$ scattering length from the shape of the Dalitz plot. Especially for the latter, the proposed analysis offers a unique approach. Another neutral decay we propose to examine is

$$\eta' \to 3\pi^0. \tag{2}$$

So far, this decay has only been observed by the GAMS collaboration. It will be possible to extract the $\pi\pi$ scattering length from this decay. We further plan to measure the branching ratio for

$$\eta' \to \gamma\gamma. \tag{3}$$

This ratio, in conjunction with $\mathrm{BR}(\eta \to \gamma\gamma)$, allows to investigate the $SU(3)$ singlet–octet mixing angle. The upper limits for the decays

$$\eta' \to \eta e^+ e^-, \tag{4}$$

$$\eta' \to \pi^0 e^+ e^-, \tag{5}$$

which are forbidden by C–invariance in first order, but allowed in second, are interesting channels we want to investigate. However, the sensitivities for charged channels have still to be determined from simulation studies. Another test of C–invariance is the branching ratio of the decay

$$\eta' \to 3\gamma. \tag{6}$$

Finally, we plan to search for the CP–forbidden decay

$$\eta' \to 4\pi^0. \tag{7}$$

The proposed experiment will use the superb properties of the Crystal Ball (CB) multiphoton spectrometer as the central detector. In the forward direction the Crystal Ball will be augmented

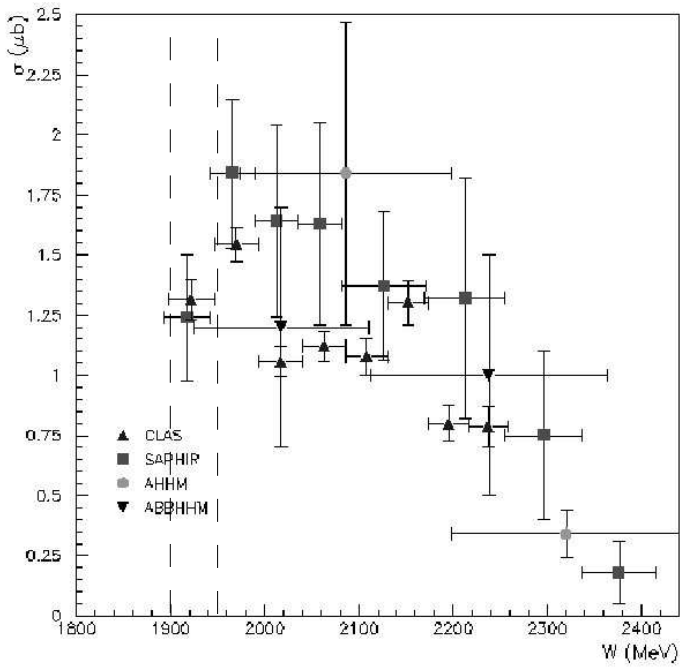

Figure 1: World data on the total cross section for η' photoproduction. The dashed lines indicate the energy region accessible with the end–point tagger at MAMI for an electron beam energy $E_e = 1.558\,\mathrm{GeV}$.

with a block of TAPS BaF_2– and $PbWO_4$–crystals. Together CB and TAPS cover roughly 97 % of the full solid angle. The whole setup has excellent energy and angular resolution and is self–triggering. These properties have shown to be extremely useful in our first precision measurements of various η decay channels at MAMI. The maximum electron energy $E_e = 1.558\,\mathrm{GeV}$ available from MAMI-C will be used. Since the standard tagging spectrometer just misses the energy region above the η' photoproduction threshold at $E_{thr} = 1.447\,\mathrm{GeV}$ ($W = 1.896\,\mathrm{GeV}$), a new tagging device is currently under construction, which covers the full energy range available for η' photoproduction at MAMI.
A feasibility study for the measurement of η' decays with the, at that time, highest available electron beam energy $E_e = 1.508\,\mathrm{GeV}$ was done in 2007. In 2008 the MAMI-C energy could be raised to $E_e = 1.558\,\mathrm{GeV}$. A preliminary analysis of these data showed an increase in statistics by a factor of 3.5 with respect to the lower energy $E_e = 1.508\,\mathrm{GeV}$. There are plans for a further upgrade of the electron beam energy to $E_e = 1.6\,\mathrm{GeV}$. Then we expect an additional increase in the η' yield by at least a factor of 2.

2 Physic Aspects

2.1 η' Photoproduction Cross Section

The existing experimental data on η' photoproduction are rather scarce. Fig. 1 summarises all data points on the total cross section of the $\gamma p \to \eta' p$ reaction. The most precise data come from the CLAS collaboration at Jefferson Lab [9] and from SAPHIR at ELSA [10]. However, the binning is large in this plot, and especially in the vicinity of the η' threshold region ($W \approx 1.896\,\mathrm{GeV}$) only one data point per experiment exists.
At MAMI in the A2 hall we have the possibility to measure the total cross section in the vicinity of the η' threshold with unprecedented precision. The two dashed lines in fig. 1 indicate the

Experiment	Reference	Statistics	α	Channel
GAMS	[12]	5400	-0.058 ± 0.013	$\eta' \to \eta\pi^0\pi^0$
GAMS	[7]	15000	-0.042 ± 0.008	$\eta' \to \eta\pi^0\pi^0$
BNL	[13]	1400	-0.08 ± 0.03	$\eta' \to \eta\pi^+\pi^-$
CLEO	[14]	6700	-0.021 ± 0.025	$\eta' \to \eta\pi^+\pi^-$
VES	[15]	7000	$-0.072 \pm 0.012 \pm 0.006$	$\eta' \to \eta\pi^+\pi^-$

Table 1: World data for the Dalitz plot parameter α of the $\eta' \to \eta\pi\pi$ decay. The two results form the GAMS collaboration stem from the decay into neutral pions. The other experiments used the $\eta' \to \eta\pi^+\pi^-$ decay to determine α.

energy range that can be examined with the new end–point tagger (see section 3.1) for the maximum MAMI-C electron energy $E_e = 1.558\,\text{GeV}$. This end–point tagger will reach a photon energy resolution $\Delta E_\gamma \approx 2.3\,\text{MeV}$. With a similar precision it was already possible to measure the total η photoproduction cross section, see ref. [11]. If the upgrade of MAMI to $E_e = 1.6\,\text{GeV}$ is successful, the region will be extended to $W = 1.97\,\text{GeV}$.
For calculating η' production rates at MAMI, we take the total cross section from the SAPHIR [10] and Jefferson Lab [9] results in fig. 1 as a basis. The average total cross section of $\gamma p \to \eta' p$ from threshold to the maximum photon energy avaliable at MAMI-C is about $1\,\mu\text{b}$.

2.2 $\eta' \to \eta\pi^0\pi^0$

The $\eta' \to \eta\pi^0\pi^0$ decay occurs by strong interactions. At low energies $\pi\pi$ and $\pi\eta$ scattering are relatively weak and appear to vary slowly. The modest energy dependence of $\pi\pi$ and $\pi\eta$ scattering gives rise to a small variation in the density of the Dalitz plot. Because the energy release in the $\eta' \to \eta\pi^0\pi^0$ decay is small, only 141 MeV, the matrix element can be described by the following formulae:

$$|M|^2 = |1 + \alpha y|^2 + dx^2 \quad \text{or} \quad |M|^2 = 1 + ay + by^2 + dx^2, \tag{8}$$

where x and y are the Dalitz variables

$$y = \frac{(2m_\pi + m_\eta)}{m_\pi} \cdot \frac{T_\eta}{Q} - 1, \tag{9}$$

$$x = \sqrt{3}\frac{(T_1 - T_2)}{Q}. \tag{10}$$

and

$$a = 2Re(\alpha) \quad \text{and} \quad b = Re^2(\alpha) + Im^2(\alpha). \tag{11}$$

Here T_1, T_2, and T_η are the kinetic energies in the η' rest frame of the two π^0 and the η, respectively; $Q = m'_\eta - m_\eta - 2m_\pi \approx 141$ MeV. For the $\eta' \to \eta\pi^0\pi^0$ decay Bose–Einstein symmetry forbids a linear term in x. A non–vanishing term cx for the $\eta' \to \eta\pi^+\pi^-$ channel would indicate C-violation.
Four experiments determined the parameter α so far (see table 1); only the GAMS collaboration used the decay channel with neutral pions [12, 7]. The experiments CB@BNL [13], VES [16] and CLEO [14] investigated the $\eta' \to \eta\pi^+\pi^-$ channel. In the analysis of the CB@BNL [13],

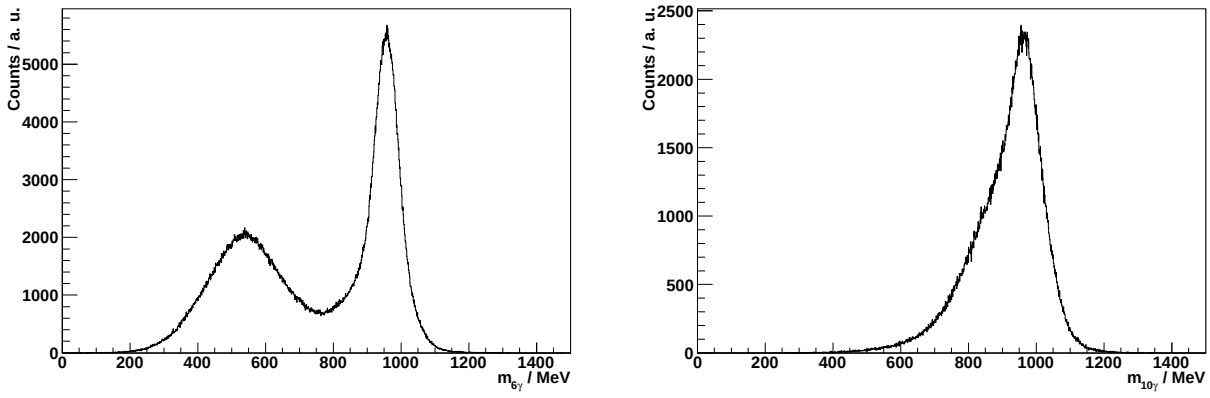

Figure 2: Simulated invariant mass spectra for the $\eta' \to \eta\pi^0\pi^0$ decay. Left: requiring 6 detected photons in the final state ($\eta \to \gamma\gamma$). Right: requiring 10 detected photons in the final state ($\eta \to 3\pi^0$).

GAMS [12] and CLEO [14] data $Im(\alpha) = 0, c = 0, d = 0$ were assumed. Although the values agree within the errors, the precision of existing data is far from being satisfactory. Both the latest GAMS analysis [7] and a re–analysis of the VES data [16] (using 20000 $\eta' \to \eta\pi^+\pi^-$ events) investigated the matrix element $|M|^2$ with the second parametrisation in 8. Also these results agree only very poorly with each other and it is not obvious, if the C–violating parameter c is consistent with zero. Clearly, high precision experimental data is needed. The proposal outlined in this paper will significantly improve the experimental situation with a data set containing one order of magnitude higher statistics than previous experiments.

The analysis of the $\eta' \to \eta\pi^0\pi^0$ decay amplitude is hampered by the occurrence of a cusp effect in the $\pi^0\pi^0$ invariant mass spectrum, due to the opening of the $\pi^+\pi^- \to \pi^0\pi^0$ charge–exchange reaction. Such a cusp effect has been investigated in $K^+ \to \pi^0\pi^0\pi^+$ decays by the NA48 collaboration with high precision. In [17] a formalism, using $\eta' \to \eta\pi^0\pi^0$ decays, has been developed to extract the $\pi\pi$ scattering lengths a_0 and a_2 from a detailed study of the shape of the Dalitz plot and the cusp. The authors of [17] predict a cusp effect of the order of 8 %. But not only the $\pi\pi$ scattering lengths influence the decay spectrum. There is the secondary final state rescattering channel $\pi\eta$. The effects of this rescattering are smaller than for the $\pi\pi$ reaction, but were systematically taken into account in [17]. Hence, a detailed study of the $\eta' \to \eta\pi^0\pi^0$ decay amplitude might also provide the possibility to obtain information about the $\pi\eta$ scattering lengths, which can hardly be measured in other reactions.

Fig. 2 shows invariant mass distributions for the $\eta' \to \eta\pi^0\pi^0$ decay for 6 million simulated events, allowing for all decay channels of the intermediate η meson. The left picture was generated for events with 6 detected photons in the final state, which corresponds mainly to the $\eta \to \gamma\gamma$ decay; in the right picture 10 detected photons were required, thus, mainly looking for the $\eta \to 3\pi^0$ channel. Both pictures show clear peaks at the η' mass of 957.78 MeV. The broad background in the left picture stems mostly from $\eta \to \pi^+\pi^-\pi^0$ events. The peak for the 10–photon case has some background at lower masses coming from energy losses and problems in the cluster reconstruction. The combined detection efficiency for both channels is $\varepsilon \approx 30\,\%$.

As mentioned above, data on the η' were measured in 2007 and 2008 with an untagged photon beam. Results of an $\eta' \to \eta\pi^0\pi^0$ analysis of these data, using kinematic fitting routines, are shown in fig. 3 [18] (left picture: $\eta \to \gamma\gamma$; right picture: $\eta \to 3\pi^0$). Both spectra show clear peaks at the η' mass with background at lower masses. With the end-point tagger, see section 3.1, we not only expect a higher event rate, but also a better event selection due to a more sophisticated trigger.

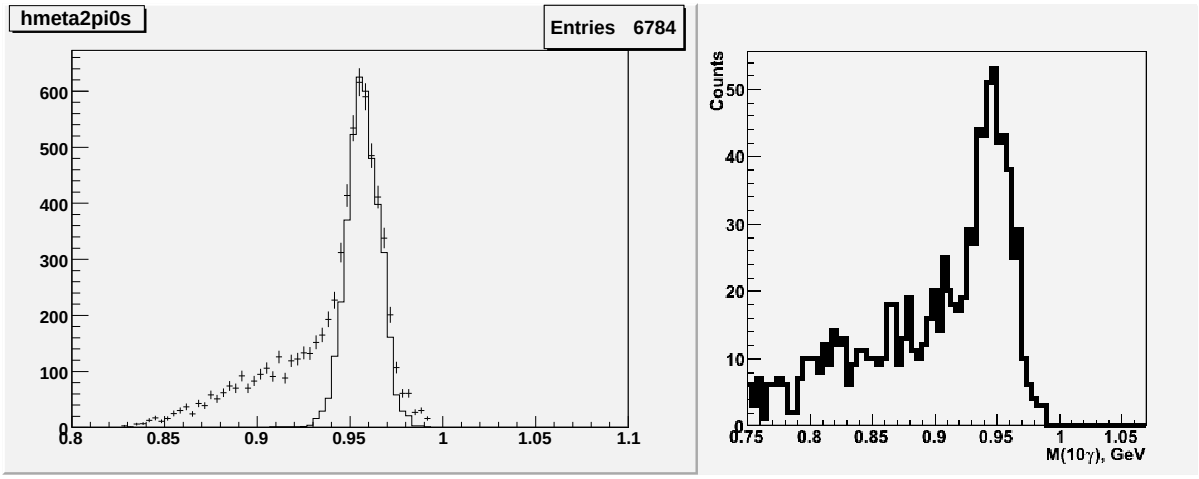

Figure 3: Invariant mass spectra for the $\eta' \to \eta\pi^0\pi^0$ decay from an analysis of data measured with the Crystal Ball at MAMI-C [18]. Left: result from the analysis of the $\eta' \to \eta(\gamma\gamma)\pi^0\pi^0$ decay. The solid line shows the result from a simulation. Right: result from an analysis of the $\eta' \to \eta(3\pi^0)\pi^0\pi^0$ channel.

2.3 $\eta' \to 3\pi^0$

The $\eta' \to 3\pi^0$ decay has a larger phase space than the $\eta' \to \eta\pi^0\pi^0$ channel, but is G–forbidden. It still occurs as a consequence of the G–violating mass term of the QCD Lagrangian with $\mathrm{BR}(\eta' \to 3\pi^0) = (1.54 \pm 0.26) \cdot 10^{-3}$. The physics of the $\eta' \to 3\pi^0$ decay is similar to $\eta' \to \eta\pi^0\pi^0$. Due to final state rescattering of the pions an energy dependence on the shape of the Dalitz plot is introduced. The matrix element for this decay can be parametrised as

$$|M|^2 \sim 1 + 2\beta Z, \tag{12}$$

where Z is the square of the distance from the center of the Dalitz plot ρ:

$$Z = X^2 + Y^2 = 6 \sum_{i=1}^{3} \left(\frac{E_i - m_{\eta'}/3}{m_{\eta'} - 3m_{\pi^0}} \right)^2 = \frac{\rho^2}{\rho_{max}^2}. \tag{13}$$

The E_i are the pion energies in the η' rest frame.
Only two measurements of the Dalitz plot parameter β exist. Both were performed by the GAMS collaboration [19, 8]. The first one ($\beta = -0.1 \pm 0.3$ [19]) was based on 40 events, while the recently published result $\beta = -0.59 \pm 0.18$ was obtained from a larger data sample of 235 ± 45 $\eta' \to 3\pi^0$ events. This latest result is 3σ away from zero. We will measure about 3600 $\eta' \to 3\pi^0$ events in 600 hours, increasing the GAMS statistics by one order of magnitude, thus, reducing the statistical uncertainty by a factor of five. Assuming a similar central value as the GAMS–result, we will measure the Dalitz plot parameter β with 10σ significance. GAMS published also a new branching ratio $\mathrm{BR}(\eta' \to 3\pi^0) = (1.8 \pm 0.4) \cdot 10^{-3}$, which we will improve by a factor of 10.
Fig. 4 shows the invariant mass for the $\eta' \to 3\pi^0$ decay for 1 million simulated events. Here, only events with six detected photons were used without any other restrictions. The mass shows a prominent peak at the η' mass and small background at lower masses. The detection efficiency for this decay is $\varepsilon \approx 25\,\%$.

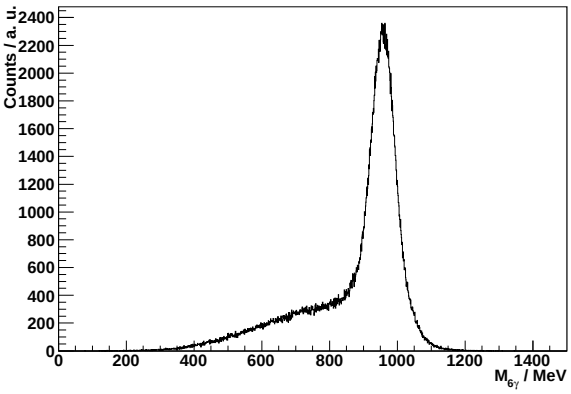

Figure 4: Simulated invariant mass spectrum for the $\eta' \to 3\pi^0$ decay.

2.4 η–η' Mixing Angle

The nonet of pseudoscalar mesons P can be described in terms of the $SU(3)$ octet and singlet matrices [21]:

$$P_8 = \begin{pmatrix} \frac{1}{\sqrt{2}}\pi^0 + \frac{1}{\sqrt{6}}\eta & \pi^+ & \mathrm{K}^+ \\ \pi^- & -\frac{1}{\sqrt{2}}\pi^0 + \frac{1}{\sqrt{6}}\eta & \mathrm{K}^0 \\ \mathrm{K}^- & \bar{\mathrm{K}}^0 & -\frac{2}{\sqrt{6}}\eta \end{pmatrix} \tag{14}$$

$$P_0 = \frac{1}{\sqrt{3}}\eta_0 I. \tag{15}$$

The physical states, η and η', are not pure SU(3)–octet and SU(3)–singlet states. The $\eta - \eta'$ mixing is usually formulated in terms of the mixing angle θ, or $\phi = \theta + \arctan(\sqrt{2})$. θ refers to the octet–singlet, and ϕ to the nonstrange–strange basis:

$$\eta = \eta_8 \cos\theta - \eta_0 \sin\theta = (u\bar{u} + d\bar{d})/\sqrt{2}\cos\phi - s\bar{s}\sin\phi \tag{16}$$

$$\eta' = \eta_8 \sin\theta + \eta_0 \cos\theta = (u\bar{u} + d\bar{d})/\sqrt{2}\sin\phi + s\bar{s}\cos\phi \tag{17}$$

The value for θ is $(-20 \pm 2)^\circ$. If we choose $\theta = -19.5^\circ$, the physical η can be parametrised as:

$$|\eta\rangle = \frac{1}{\sqrt{3}}|u\overline{u} + d\overline{d} - s\overline{s}\rangle, \tag{18}$$

which means that the η is an eigenstate of the I, U, and V operators of SU(3) [22]. In this parametrisation the η' is $|\eta'\rangle = \sin\theta|\eta_8\rangle + \cos\theta|\eta_0\rangle = \frac{1}{\sqrt{6}}|u\overline{u} + d\overline{d} + 2s\overline{s}\rangle$ and has twice the s–quark content of the η.
Because each of the physical states, η and η', has both singlet and octet components, in a more evolved parametrisation two mixing angles are introduced and one defines four independent decay constants [23]:

$$\begin{pmatrix} f_\eta^8 & f_\eta^0 \\ f_{\eta'}^8 & f_{\eta'}^0 \end{pmatrix} = \begin{pmatrix} f_8\cos\theta_8 & -f_0\sin\theta_0 \\ f_8\sin\theta_8 & f_0\cos\theta_0 \end{pmatrix}. \tag{19}$$

Using this approach, it is possible to calculate the decay widths for the $\eta \to \gamma\gamma$ and $\eta' \to \gamma\gamma$ decays, as shown in [23]. In this calculation four unknown parameters $(\theta_8, \theta_0, f_8, f_0)$ appear. To determine these values one needs additional experimental constraints as the decay widths of the $\eta \to \gamma\gamma$ and $\eta' \to \gamma\gamma$ decays. By measuring these two decays and improving the accuracies of the widths we can give an important input for the determination of the mixing angles θ_8 and θ_0.

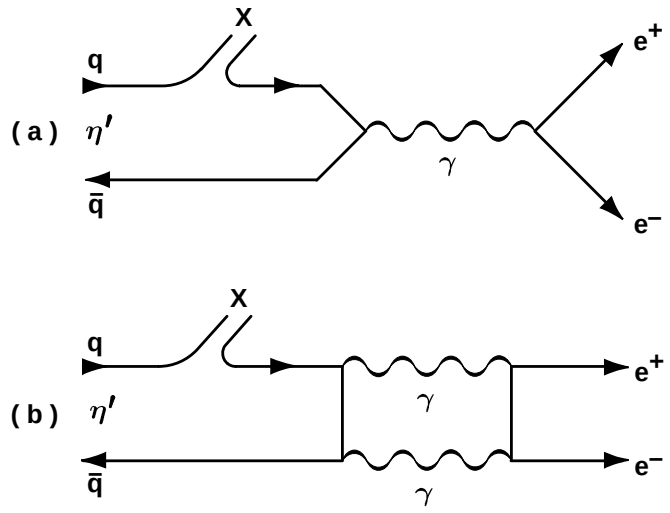

Figure 5: (a) C–violating (BR$\sim \alpha^2$) and (b) C–conserving (BR$\sim \alpha^4$) contributions to the decay $\eta' \to Xe^+e^-$, where X is an η or π^0 [14].

Recently the KLOE collaboration published data on the η–η' mixing angle and a possible gluonium content to the η' [24, 26] determined from $R = \Gamma(\phi \to \eta\gamma)/\Gamma(\phi \to \eta'\gamma)$. They found a non–zero gluonium content to the η', contrary to the theoretical calculation in [25]. Further investigations of the η–η' mixing scheme are needed and precise data from experiments with the Crystal Ball at MAMI will give important input to these investigations. The uncertainty of the width of the $\eta' \to \gamma\gamma$ decay, which is of the order of 10 %, is currently determined by both the uncertainty of the branching ratio and the uncertainty of the total width of the η'. With the expected 40000 events in 600 hours of data taking, we will reduce the uncertainty of BR$(\eta' \to \gamma\gamma)$ down to the 1 % level. Then the uncertainty of $\Gamma(\eta' \to \gamma\gamma)$ will be dominated by the error of the total η' width.

2.5 Symmetry Violaton in η' Decays

C–invariance, or charge conjugation symmetry, is the invariance of a system to the interchange of the colored quarks with their antiquarks of anticolor, the charged leptons with their antileptons, the left(right)-handed neutrinos with the left(right)-handed antineutrinos, and vice versa. C–invariance holds for all purely electromagnetic and all strong interactions, but the experimental limits are not extremely strong. The Review of Particle Physics [20] lists the most important weak and electromagnetic decays whose observation would violate conservation laws. Fourteen tests of C–invariance are listed: six involve decays of the η, five of the η', two of the ω and one of the π^0. Because the width of the η' is broader than the η, η' decays are less sensitive to C–violation than the corresponding η decays.
The η', η and π^0 are even eigenstates of C, while a photon is C–odd; thus, the one–photon process will be C–violating and the two–photon process C–conserving. The decays $\eta' \to \eta e^+e^-$ and $\eta' \to \pi^0 e^+e^-$ can occur with one (C–violating) or two (C–conserving) intermediate virtual photons, as shown in fig. 5 [14]. Cheng has estimated the relative rate for the C–conserving part of the amplitude for the similar decay $\eta \to \pi^0 e^+e^-$: BR$(\eta \to \pi^0 e^+e^-)$/BR$(\eta \to \pi^0\gamma\gamma) \approx 10^{-5}$ [27]. The branching ratio of $\eta' \to \pi^0\gamma\gamma$ is $< 8 \times 10^{-4}$. Assuming a similar ratio for the η' decays, a signal at the 10^{-9} level or larger would signify a large C-violating contribution or other New Physics. The current 90% confidence upper limits for these decays are BR$(\eta' \to \eta e^+e^-) < 2.4 \times 10^{-3}$ and BR$(\eta' \to \pi^0 e^+e^-) < 1.4 \times 10^{-3}$ [14]. If these branching ratios were true, we would expect approximately 3000 events in 600 hours for each decay. Thus, we can

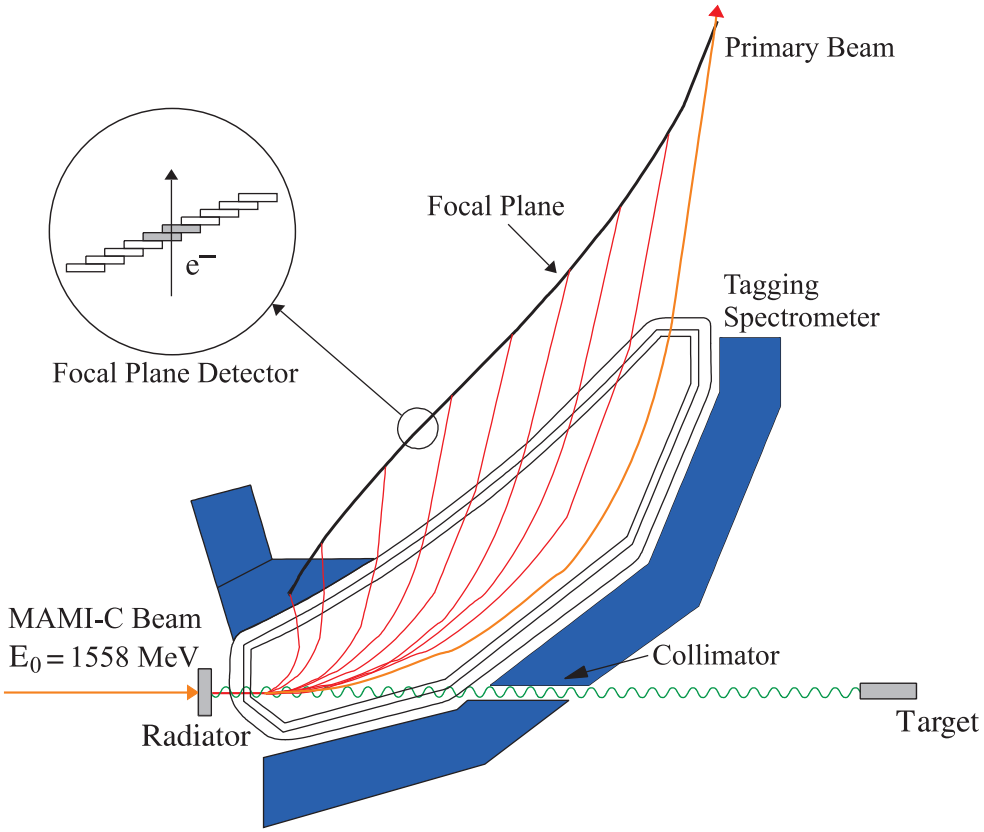

Figure 6: The Glasgow tagged photon spectrometer

improve these upper limits by more than an order of magnitude.
The $\eta' \to 3\gamma$ decay is rigorously forbidden by C–invariance. This decay should be small as it is a third order electromagnetic interaction and $\alpha^3 = 4 \cdot 10^{-7}$. The rate is further suppressed by substantial factors coming from phase space and angular momentum barrier considerations [28]. The $\eta' \to 3\gamma$ decay can be isoscalar or isovectorial or can even occur via the hypothetical isotensor interaction. The Particle Data Group [20] lists the upper limit for the $\eta' \to 3\gamma$ branching ratio as $1 \cdot 10^{-4}$. We can improve this upper limit substantially.
The PDG [20] lists for the CP–forbidden $\eta' \to 4\pi^0$ decay a branching ratio $\mathrm{BR}(\eta' \to 4\pi^0) < 5 \cdot 10^{-4}$. This decay is also P–violating. Investigating this decay will be a very interesting test of conserving symmetries. We will improve the upper limit of this decay at least by one order of magnitude.
The decay $\eta' \to e\mu$ with no accompanying neutrinos is an example of lepton number violation. The theoretical upper bound for this decay is on the order of 10^{-11}, calculated from the experimental limit on $\mu^- \to e^-$ conversion in heavy nuclei [29]. The current upper limit for this decay is $\mathrm{BR}(\eta' \to e\mu) < 4.7 \cdot 10^{-4}$ [14]. Furthermore, second class weak interactons in $\eta' \nrightarrow \pi^0 l\nu$ and $\eta' \nrightarrow \pi^0 \mu e$ will be studied.

3 Experimental Apparatus

3.1 End–point Tagger

The A2 photon beam is derived from the production of Bremsstrahlung photons during the passage of the MAMI electron beam through a thin radiator. The Glasgow tagged photon spectrometer [30, 31] (fig. 6) provides energy tagging of the photons by detecting the post–radiating electrons. It can determine the photon energy with a resolution of 2 to 4 MeV depending on

the incident beam energy, with a single–counter time resolution $\sigma_t = 0.17\,\text{ns}$ [32]. Each counter can operate reliably to a rate of $\sim 1\,\text{MHz}$, giving a photon flux of $2.5 \cdot 10^5\,(\text{s MeV})^{-1}$. Photons can be tagged in the momentum range from 4.7 to 93.0 %. This means that the highest tagged photon energy, at an electron beam energy of $E_e = 1558\,\text{MeV}$, is $E_\gamma \approx 1448\,\text{MeV}$.
Since the η' photoproduction threshold is at $E_{thr} \approx 1447\,\text{MeV}$, almost the full photon energy range accessible at MAMI for η' production is not covered by the Glasgow tagged photon spectrometer. Therefore, a new tagging device (end–point tagger) is currently constructed that will detect post–radiating electrons with energies between $E_e = 10\,\text{MeV}$ and $E_e = 150\,\text{MeV}$. Under the defined conditions these energies correspond to photon energies between $E_\gamma = 1548\,\text{MeV}$ and $E_\gamma = 1408\,\text{MeV}$. There are plans to upgrade MAMI to reach electron energies of $E_e = 1600\,\text{MeV}$. Then photon energies between $E_\gamma = 1590\,\text{MeV}$ and $E_\gamma = 1450\,\text{MeV}$ can be tagged. Thus, at least 100 MeV above the η' photoproduction threshold will be covered by the end–point tagger, which will have an energy resolution $\Delta E_\gamma \approx 2.3\,\text{MeV}$.
To study the neutral decays of the η' meson, the end–point tagger is essential for a clean trigger. So far, we measured already η' mesons, but the identification relied on the detection of the protons, which mostly hit TAPS (see below). TAPS is suitable for measuring photons, but the identification of protons is not very efficient. With the end–point tagger the detection and identification of the protons would not be required any more and, in addition, the beam rate could be increased due to a more precise trigger.
Note, that not only the η' photoproduction threshold falls within the range of the end–point tagger, but also the production thresholds of the scalar mesons $a_0(980)$ and $f_0(980)$. Further we expand into strangeness production; e.g. the maximum of $\Lambda(1405) \rightarrow \pi^0\Sigma^0$, which is at 1454 MeV, will be in the range of the end–point tagger.

3.2 Crystal Ball Detector System

The central detector system, surrounding the 10 cm long liquid hydrogen target (see fig. 7), consists of the Crystal Ball calorimeter (CB) combined with a barrel of scintillation counters for particle identification. The CB is a highly segmented 672-element NaI(Tl), self triggering photon spectrometer constructed at SLAC in the 1970's. Each element is a 41 cm (15.7 radiation lengths) long truncated triangular pyramid. They are all read out by individual photomultipliers. The CB has an energy resolution of $\Delta E/E = 0.020(E[\text{GeV}])^{0.36}$, an angular resolution in σ_θ of $2-3^\circ$ and σ_ϕ of $\sigma_\theta/\sin\theta$ for electromagnetic showers [33]. The readout electronics for the Crystal Ball were completely renewed in 2003 and are now fully equipped with SADCs, which allow for the full sampling of pulse-shape element by element. In normal operation, the onboard summing capacity of these ADCs is used to enable dynamic pedestal subtraction and the provision of pedestal, signal and tail values for each element event-by-event. Each CB element is also newly equipped with multi-hit CATCH TDCs. The readout of the CB is effected in such a way as to allow for flexible triggering algorithms. There is an analogue sum of all ADCs, allowing for a total energy trigger, and also an OR of groups of sixteen crystals to allow for a hit-multiplicity second-level trigger - ideal for use when searching for high multiplicity final states as the two important decays $\eta' \rightarrow \eta\pi^0\pi^0$ and $\eta' \rightarrow 3\pi^0$ are.
In order to distinguish between neutral and charged particles species detected by the Crystal Ball, the system is equipped with PID 2, a barrel detector of twenty-four 50 mm long 4 mm thick scintillators, arranged so that each PID 2 scintillator subtends an angle of 15° in ϕ. By matching a hit in the PID 2 with a corresponding hit in the CB, it is possible to use the locus of the ΔE, E combination to identify the particle species (fig. 8). This is primarily used for the separation of charged pions, electrons and protons. The PID 2 covers from 15° to 159° in θ.
This central system, comprising the CB and the PID 2, provides position, energy and timing information for both charged and neutral particles in the region between 21° and 159° in the polar angle, θ, and over almost the full azimuthal (ϕ) range. The excellent CB position resolution

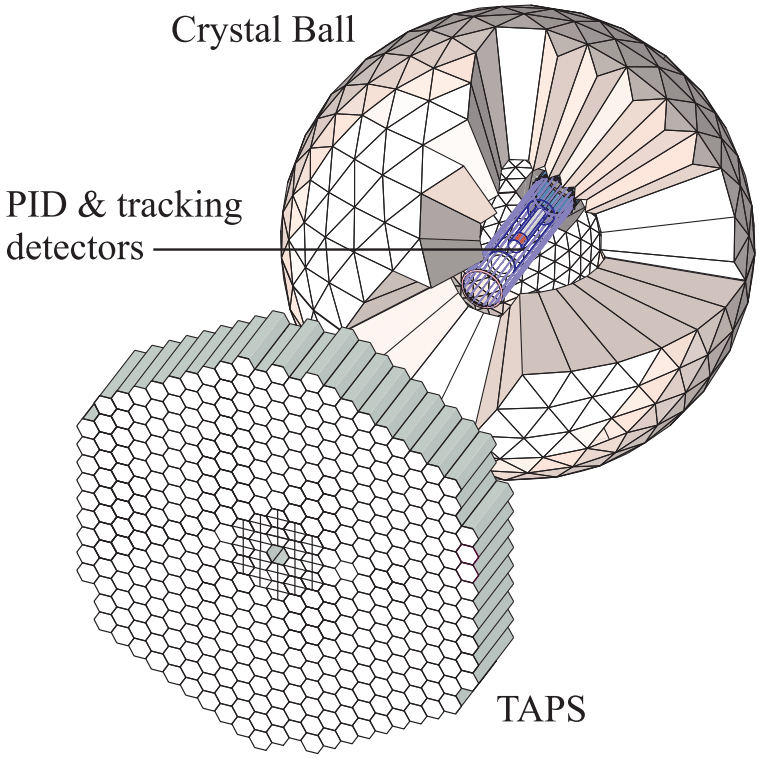

Figure 7: The A2 detector setup: the Crystal Ball calorimeter with cut–away section showing the inner detectors and the TAPS forward wall. The shown tracking detectors will not be used for the investigation of the η' decays. The inner two rings of TAPS are made of $PbWO_4$ crystals.

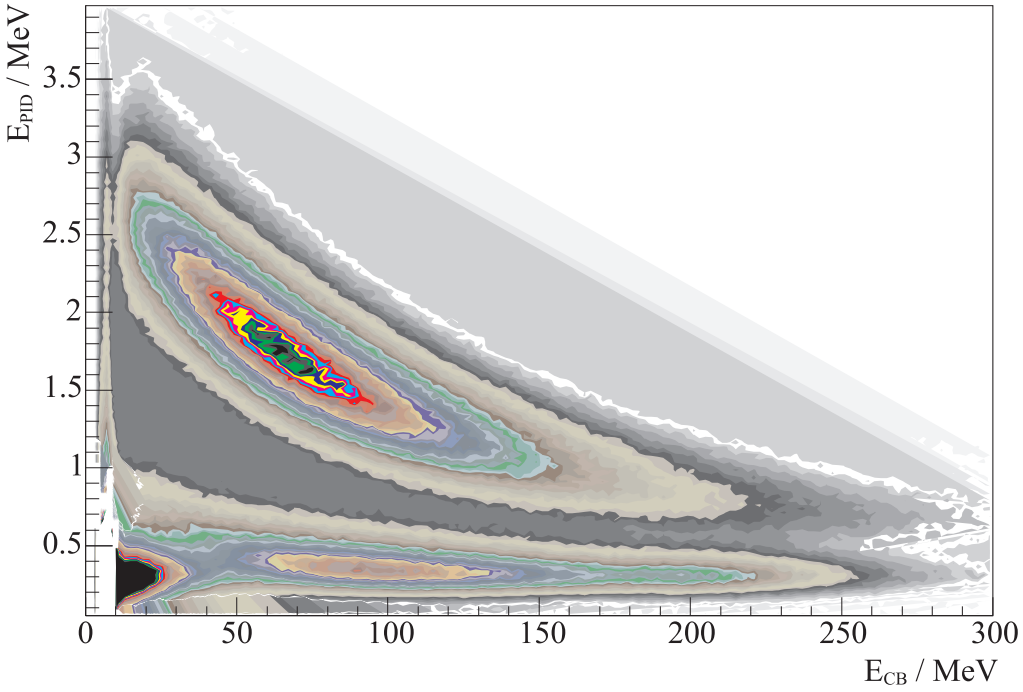

Figure 8: A typical ΔE/E plot from the PID detector. The upper curved region is the proton locus, the lower region contains the pions and the peak towards the origin contains mostly electrons.

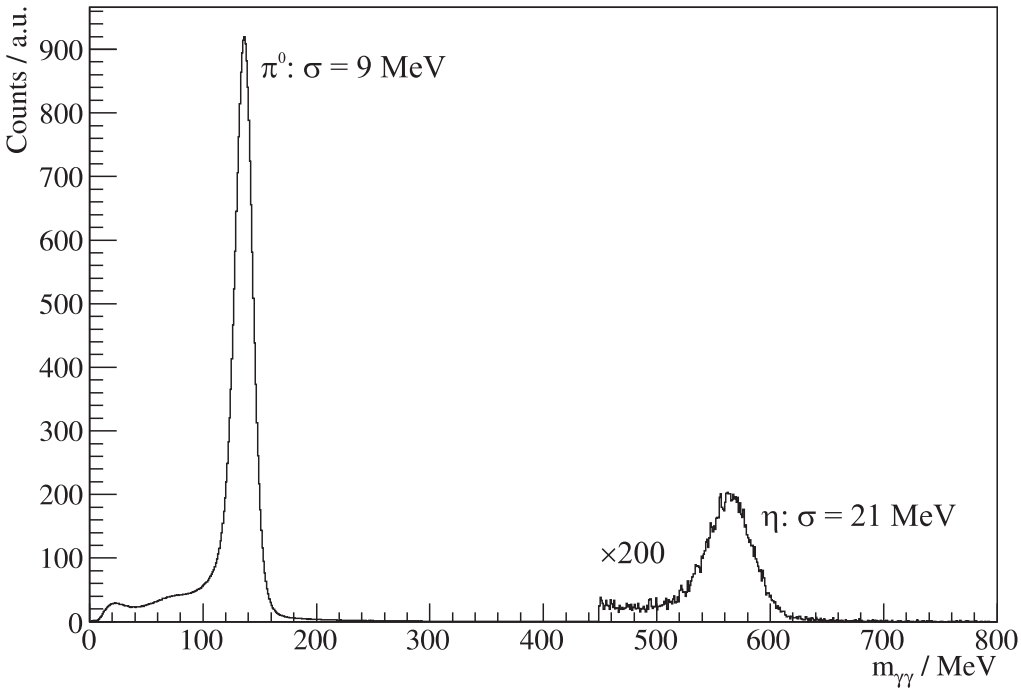

Figure 9: Two gamma invariant mass spectrum for the CB TAPS detector setup. Both η and π^0 mesons can be clearly seen.

for photons stems from the fact that a given photon triggers several crystals, and the energy-weighted mean of their positions locates the photon position to better than the crystal pitch. For charged particles which deposit their energy over only one or two crystals, this is not so precise. In fig. 9 a measured two-photon invariant mass spectrum is shown, demonstrating the good CB mass–resolution for neutral pions and η mesons.

3.3 TAPS Forward Wall

At forward angles, less than 21°, reaction products are detected in a wall consisting of TAPS BaF_2 crystals. The full detector system, as shown in fig. 7, is almost hermetic. The TAPS forward wall is composed of 384 BaF_2 elements, each 25 cm in length (12 radiation lengths) and hexagonal in cross section, with a diameter of 59 mm. Every TAPS element is covered by a 5 mm thick plastic veto scintillator. The single counter time resolution is $\sigma_t = 0.2$ ns. The energy resolution can be described by $\Delta E/E = 0.018 + 0.008/(E[\mathrm{GeV}])^{0.5}$ [33]. The angular resolution in the polar angle is better than 1°, and in the azimuthal angle it improves with increasing θ, being always better than 1/R radian, where R is the distance in centimeters from the central point of the TAPS wall surface to the point on the surface where the particle trajectory meets the detector. The TAPS readout was custom built for the beginning of the CB@MAMI program and is effected in such a way as to allow particle identification by Pulse-Shape Analysis (PSA), Time-of-Fight (TOF) and $\Delta E/E$ methods (using the energy deposit in the plastic scintillator to give ΔE). TAPS can also contribute to the CB multiplicity trigger and is currently divided into upto six sectors for this purpose.
The 2 inner rings of 18 BaF_2 elements have been replaced recently by 72 $PbWO_4$ crystals each 20 cm in length (22 radiation lengths), see fig. 7. The higher granularity improves the rate capability as well as the angular resolution. The crystals are operated at room temperature. The energy resolution for photons is similar to BaF_2 under this condition [34].

4 Beamtime Request

The proposed experiment will use the highest electron beam energy available at MAMI–C. Using the end–point tagger, currently under construction, the $PbWO_4$ crystals in TAPS and a thick radiator for producing the Bremsstrahlung photons, a conservative estimate gives the following parameters:

- Incoming electron beam energy: $E_e = 1558\,\mathrm{MeV}$,
- Tagged photon energy range: $E_\gamma = 1447 - 1548\,\mathrm{MeV}$, thus $\Delta E_{tagg} \approx 100\,\mathrm{MeV}$,
- Photon flux: $N_\gamma = 10^5 \frac{1}{\mathrm{s\,MeV}}$,
- Number of protons in a 10 cm long lH_2 target: $N_t = 4.3 \cdot 10^{23}\,\mathrm{cm}^{-2}$,
- Average η' photoproduction cross section in tagged range (fig. 1): $\bar{\sigma}(\gamma p \to \eta' p) \approx 1\,\mu\mathrm{b}$.

The resulting number of η' events per hour is:

$$N_{\eta'} = \Delta E_{tagg} \cdot N_\gamma \cdot N_t \cdot \bar{\sigma}(\gamma p \to \eta' p) \cdot 3600\,\mathrm{s} \approx 15 \cdot 10^3. \tag{20}$$

With a detection efficiency $\varepsilon \approx 30\,\%$ for the $\eta' \to \eta\pi^0\pi^0$ decay, a data acquisition livetime of 80 % and $\mathrm{BR}(\eta' \to \eta\pi^0\pi^0) = (20.7 \pm 1.2)\,\%$ we expect at least 700 measured $\eta' \to \eta\pi^0\pi^0$ events per hour. For the $\eta' \to 3\pi^0$ decay with $\mathrm{BR}(\eta' \to 3\pi^0) = (1.54 \pm 0.28) \cdot 10^{-3}$ and the same acceptance and livetime we will collect 6 events per hour. In order to improve the currently highest–statistic results of the GAMS collaboration [7, 8] by one order of magnitude, a beamtime of 215 hours is needed. We request 600 hours of η' production data taking. As described above, with this beamtime we can achieve the following objectives:

- Dalitz plot: improving the precisions of the slope parameters from 3σ to at least the 10σ level,
- η–η' mixing: measurement of $\mathrm{BR}(\eta' \to \gamma\gamma)$ with a statistical uncertainty below 1 %,
- C– and CP–violation: improvement of upper limits of several decays by at least one order of magnitude.

First data taking with the possibility to extract η' mesons were already measured with low statistics. From this experience, the trigger and setup conditions are already known. Thus, only 50 hours for setting up the end–point tagger are needed. Additionally, we need 200 hours for empty target measurements and background studies. We request a total beamtime for the η' experiment of

850 Hours.

A Competition in η' Physics

As discussed above, the η' meson is a unique laboratory for the study of the $\pi - \pi$ and $\pi - \eta$ interactions, for precision tests of C– and CP–invariance, as well as for a test of chiral perturbation theory. At MAMI–C with the increased beam energy of 1558 MeV and the Crystal Ball/TAPS setup, a perfect environment for η' studies is given. The high statistics achievable at MAMI together with the good signal-to-background conditions makes investigations of the η' meson especially competitive at MAMI. In this chapter we discuss the competitors in the field of η and η' decays. These are the KLOE experiment at the DAΦNE collider, the Crystal Barrel detector at ELSA and WASA at COSY. Also other experiments, like BES III and GAMS, are capable of measuring η' decays, but knowledge about plans of these groups in this field is scarce. We will see that at MAMI–C the potential is given to become the leading research laboratory for η' mesons.

A.1 KLOE at DAΦNE

The experiment KLOE is located at the Frascati ϕ-factory DAΦNE, an e^+e^- collider running at a fixed c. m. energy of $\sqrt{s} = 1.02\,\mathrm{GeV}$, corresponding to the mass of the ϕ meson. The total cross section for ϕ production at the DAΦNE c. m. energy of $\sqrt{s} = 1.02\,\mathrm{GeV}$ is about $3.3\,\mu\mathrm{b}$ [35]. The branching ratio of the decay $\phi \to \eta'\gamma$, in which η' mesons are produced, is $6 \cdot 10^{-5}$.
KLOE is an almost 4π acceptance detector, designed to measure the momentum and directions of charged particles as well as the energy and direction of photons. It consists of the world's largest cylindrical drift chamber placed in a magnetic field of 0.6 Tesla and a spaghetti-type electromagnetic calorimeter made of a matrix of scintillating fibers embedded in lead. The z-position and, therefore, the polar angle of a hit is determined using the Time–of–Flight information from opposite sides of the scintillating fibers. The energy resolution of the calorimeter is $\sigma_E/E = 5.7\%/\sqrt{E(\mathrm{GeV})}$. The θ resolution is determined by the TOF resolution, which is $\sigma_t = 54(\mathrm{ps})\sqrt{E(\mathrm{GeV})}$.
Between 2000 and 2005 KLOE has collected an integrated luminosity of roughly $2.5\,\mathrm{fb}^{-1}$. This corresponds to about $5 \cdot 10^5$ produced η' mesons. In the meantime the luminosity of the DAΦNE collider has been increased by roughly a factor 3. In autumn of 2009 first runs with the improved accelerator DAΦNE are planned (KLOE phase-2). The future staged programme of KLOE forsees first to reach an integrated luminosity of $5\,\mathrm{fb}^{-1}$ within one year with the current detector setup. Afterwards, KLOE will be upgraded with a new inner tracker system, $\gamma\gamma$-tagger(s) and new small angle calorimeter(s) [37]. After this upgrade, the KLOE collaboration plans to collect within three to four years an integrated luminosity of 40 to $50\,\mathrm{fb}^{-1}$.
The method of η and η' tagging at KLOE is based on the detection of the radiative photon from the ϕ decay. This recipe works very well for cases when the radiative photon can be reliably separated from other decay particles. For example, in the case of $\phi \to \eta\gamma \to 3\pi^0\gamma$ decay the energy of the radiative photon is about 363 MeV, while the average energy of photons from the η decay is only ca. 100 MeV. The situation is more complicated for η' mesons. In the case of the $\phi \to \eta'\gamma$ decay the radiative photon is about 60 MeV and can hence be easily misidentified with photons from the $\eta' \to \eta\pi^0\pi^0$ or $\eta' \to 3\pi^0$ processes. Moreover, the relatively poor energy and space resolution of the KLOE electromagnetic calorimeter worsens the possibility of finding a proper combination of the photons needed to reconstruct the π^0's and η's from the η' decay. Such a reconstruction will be the key in order to obtain accurate results for the Dalitz plots analyses of the $\eta' \to \eta\pi^0\pi^0$ and the $\eta' \to 3\pi^0$ decays.
We conclude that despite the fact that the KLOE collaboration has a large η' sample in hand and will significantly increase this sample in future, the environment at MAMI with the Crystal Ball setup seems preferable for multiphoton η' decays. For what concerns the available statistics, only in a few years, when the KLOE phase-2 program will be successfully performed, KLOE will be able to compete with the MAMI–C statistics.

In Novosibirsk a collider running in the ϕ mass region is in the commissioning phase (VEPP-2000 project). Differently from DAΦNE, it is however not foreseen that the collider will run on the ϕ peak for a longer period. Moreover, the design luminosity on the ϕ peak will be lower than at DAΦNE. No competitive results concerning η' decays can hence be expected from the experiments CMD-III and SND, which are located at VEPP-2000.

A.2 WASA at COSY

A significant part of the new WASA at COSY experimental programme is dedicated to studies of η and η' decays. In 2006 the commissioning of WASA at the COSY proton ring started. The calculated η' production rate at COSY in proton–proton collisions is about 30 η' per second and, therefore, a factor 7 higher than at MAMI–C. The WASA detector is well suited to detect the energy and direction of photons as well as the momenta and directions of charged particles. However, the feasibility of the η' program at COSY still needs to be proven. The similar WASA programme at the CELSIUS proton machine at Uppsala suffered from serious complications such as the stability of the pellet target, very large hadronic background and beam associated backgrounds. Those issues were never fully resolved at CELSIUS and the COSY setup now faces similar problems [38]. First reliable η' production data are expected for 2011. It is however still not clear, if the proposed η' production rate can be achieved.
The WASA detector is equipped with the high resolution central magnetic spectrometer. This device makes WASA a unique setup to study charged decays of η and η'. On the other hand, the central tracker introduces about 0.2 of the radiation length worth of material between the target and the WASA electromagnetic calorimeter. For multi–photon final states, such as $\eta' \to \eta\pi^0\pi^0$ for example, the probability to loose one of the six photons due to photon conversion in the material is about 50 %. For this reason, the Crystal Ball detector is a superior device to deal with multi–photon η and η' decays.

A.3 Crystal Barrel at ELSA

The *Electronen Stretcher Anlage* (ELSA) at the University of Bonn provides an electron beam with energies up to 3.2 GeV. The electron beam is used to produce a tagged Bremsstrahlung beam with photon energies in the range from 20 to 96 % of the electron beam energy. The ELSA beam energy is high enough to cover the entire maximum of the $\gamma p \to \eta' p$ total cross section shown in fig. 1. The intensity of the ELSA photon beam can be estimated to be about $2.5 \cdot 10^4 \frac{1}{\mathrm{s\,MeV}}$ in the region between 1.45 to 3.0 GeV. The photon flux is limited by the intensity of the external electron beam which can be extracted from ELSA.
At the ELSA photon beam the CERN Crystal Barrel detector, which has a similar concept as the Crystal Ball, is used. The CsI crystals of the Crystal Barrel detector are equipped with photodiodes. Thus, the trigger solutions used for the Crystal Barrel experiment rely on TAPS and the Forward Plug detector, which is a forward wall made of a limited number of CsI crystals equipped with PMTs. Such triggering method limits the apparatus acceptance to a value, which is two to three times smaller than for the Crystal Ball.
An estimated rate for the η' photoproduction at ELSA is about 7500 $\frac{1}{\mathrm{h}}$. This is about a factor of 2 less than the estimated η' flux for the Crystal Ball experiment at MAMI–C. The limited detector acceptance due to the trigger further reduces the number of η' mesons that can be measured at ELSA by a factor two to three. Although at ELSA a much longer tagging range is used, the η' production rates show that they can hardly compete with MAMI.

A.4 Other Experimental Facilities Capable of Producing η'

The CLEO collaboration at the e^+e^- collider CESR has recently published a new result on the slope parameter of the $\eta' \to \pi^+\pi^-\eta$ decay. Previously, upper limits on the C–forbidden decays

$\eta' \to e^+e^-\pi^0$ and $\eta' \to e^+e^-\eta$ have been published. The experiment used $3.11\,\mathrm{fb}^{-1}$ of data taken on the $\Upsilon(4S)$ resonance at $\sqrt{s}$=10.58 GeV, and $1.69\,\mathrm{fb}^{-1}$ at 10.52 GeV. Approximately $(15 \pm 3)\,\%$ of the η' sample came from $B\bar{B}$ decays. Charged particle momenta were measured in a 67-layer tracking system immersed in a 1.5 T solenoidal magnetic field. The main drift chamber also determined track specific ionization (dE/dx), which aided in particle identification. A 7800-crystal CsI calorimeter detected photons, and was the primary tool for electron identification [39]. The total number of detected $\eta' \to \pi^+\pi^-\eta$ decays was about 6700 with roughly 3 % acceptance. But the invariant mass distribution of the $\pi^+\pi^-\eta$ event showed significant (about 50 %) background under the η' peak. CLEOs data collection ended on March 31, 2008 [39] and no further data taking will take place in future.

Experience from the CLEO collaboration was in the meantime transferred to the BES-III [39] project. The BES-III detector is located at the e^+e^- collider BEPC-II in Beijing, a so-called τ-charm-factory. In mid-2008, the BEPC-II/BES-III setup started operation at center-of-mass energies $\sqrt{s} = 2.0 - 4.6\,\mathrm{GeV}$ [40] with peak luminosities of up to 10^{32} $\mathrm{cm}^{-2}\mathrm{s}^{-1}$ reached in 2009. The design luminosity in this energy region ranges from $1 \cdot 10^{33}$ $\mathrm{cm}^{-2}\mathrm{s}^{-1}$ down to about $0.6 \cdot 10^{33}$ $\mathrm{cm}^{-2}\mathrm{s}^{-1}$ at lower energies. In a one year's running period (10^7 s) it is possible to collect an integrated luminosity of $3\,\mathrm{fb}^{-1}$ on the J/ψ peak at design luminosity. Ref. [40] describes the possibilities for η and η' physics with BES-III based on such a data set. According to this study, ca. 61 million η' mesons can be collected from radiative and hadronic J/ψ decays. So far, we are not aware of any plans to launch an η' program with BES-III. Furthermore, it has to be proven that the luminosities, stated in [40], can be achieved and that the background conditions can be kept under control.

η' mesons can also be produced in charge-exchange reactions at high-energy hadron colliders. The GAMS collaboration (Protvino, Russia) published recently results [7, 8] on the $\eta' \to 3\pi^0$ decay and the $\eta' \to \eta\pi^0\pi^0$ matrix element. Already from the statistical point of view, this collaboration cannot be considered as a competitor for MAMI C. We are not aware of any further improvements on the GAMS detector or the IHEP accelerator in order to increase their η' statistics.

References

[1] J. L. Goity, A. M. Bernstein, and B. R. Holstein, Phys. Rev. D **66**, 076014 (2002).

[2] M. J. Ramsey-Musolf and M. B. Wise, Phys. Rev. Lett. **89**, 041601 (2002).

[3] B. V. Martemyanov and V. S. Sopov, Phys. Rev. D **71**, 017501 (2005).

[4] A. G. Nicola and J. R. Pelaez, Phys. Rev. D **65**, 054009 (2002).

[5] P. Herczeg, Phys. Rev. D **51**, 136 (1995)

[6] B. M. K. Nefkens, Few–Body Syst. Suppl. **9**, 193 (1995).

[7] A.M. Blik *et al.*, Phys. Atom. Nucl. **72**, 231 (2009).

[8] A.M. Blik *et al.*, Phys. Atom. Nucl. **71**, 2124 (2008).

[9] M. Dugger *et al.*, Phys. Rev. Lett. **96**, 062001 (2006).

[10] R. Plotzke *et al.*, Phys. Lett. B **444**, 555 (1998).

[11] M. Unverzagt *et al.*, Eur. Phys. J. A **39**, 169 (2009).

[12] D. Alde *et al.*, Phys. Lett. b **177**, 115 (1986).

[13] G.R. Kalbfleisch, Phys. Rev. D **10**, 916 (1974).

[14] R. Briere *et al.*, Phys. Rev. Lett. **84**, 26 (2000).

[15] D. Amelin *et al.*, Phys. Atom. Nucl. **68**, 372 (2005).

[16] V. Dorofeev *et al.*, Phys. Lett. B **651**, 22 (2007).

[17] B. Kubis, S.P. Schneider, arXiv:0904.1320 [hep-ph].

[18] By courtesy of S. Prakhov (UCLA).

[19] D.M. Alde *et al.*, Z. Phys. C **36**, 603 (1987).

[20] C. Amsler *et al.*, Phys. Lett. B **667**, 1 (2008).

[21] L. Ametller, *Eta Physics Handbook*, Physica Scripta **T99**, 45 (2002).

[22] B.M.K. Nefkens and J.W. Price, *Eta Physics Handbook*, Physica Scripta **T99**, 114 (2002).

[23] R. Escribano and J.-M. Frére, JHEP **0506**, 029 (2005).

[24] F. Ambrosino *et al.*, Phys. Lett. B **648**, 267 (2007).

[25] R. Escribano and J. Nadal, JHEP **05**, 006 (2007).

[26] B. DiMicco (KLOE collaboration), Eur. Phys. J. A **38**, 129 (2008).

[27] T.P. Cheng, Phys. Rev. **162**, 1734 (1967).

[28] F. Berends, Phys. Lett. **16**, 178 (1965).

[29] P. Herczeg, in *Rare Decays of Light Mesons*, edited by B. Mayer (Editions Frontiers, Gif-sur-Yvette), 1990.

[30] I. Anthony, J.D. Kellie, S.J. Hall, G.J. Miller, J. Ahrens. Nucl. Instrum. Methods A **301**, 230 (1991).

[31] S.J. Hall, G.J. Miller, R. Beck, P. Jennewein, Nucl. Instrum. Methods A **368**, 698 (1996).

[32] J.C. McGeorge *et al.*, Eur. Phys. J. A **37**, 129 (2008).

[33] S. Prakhov *et al.*, Phys. Rev. C **79**, 035204 (2009).

[34] R. Novotny *et al.*, Nucl. Instrum. Meth. A **486**, 131(2002).

[35] B. DiMicco (for the KLOE Collaboration), talk on the EtaNetwork meeting, Frascati, June 13, 2005.

[36] C. Bini (for the KLOE Collaboration), Proceedings of the 34th International Conference on High Energy Physics, Philadelphia, 2008, arXiv:0809.5004 [hep-ex].

[37] P. Rossi (KLOE Collaboration), talk on "MAMI and beyond" Conference, Mainz, April 2nd, 2009, *http://www.kph.uni-mainz.de/T/MAMIandBeyond/04 Donnerstag/04 Rossi.pdf.*

[38] M. Wolke (WASA at COSY Collaboration), talk on "PrimeNet" Meeting, INFN Frascati, April 8th, 2009, *http://agenda.infn.it/conferenceDisplay.py?confId=1123.*

[39] R.A. Briere *et al.*, Expression of Interest for Expanded U.S. Participation in the Charm Physics Program of BES III, http://www.hep.umn.edu/des3/BES3_EOI_v4.pdf, September 21st, 2007.

[40] H.-B. Li, arXiv:0902.3032v2 [hep-ex], 2009.